SOLUTION OF QUASI INCOMPRESSIBLE FLOWS USING A STABILIZED FINITE ELEMENT METHOD

Perinaldo Severino Júnior, perinaldojr@yahoo.com.br
Universidade Federal de Pernambuco
Av. Prof Luiz Freire nº 1000
50740-540 Recife, PE. Brazil

Gustavo Koury Costa, gustavokoury@cefetpe.br
Centro Federal de Educação Tecnológica de Pernambuco
Av. Prof Luiz Freire nº 500
50740-540 Recife, PE. Brazil

Carlos Alberto Brayner de Oliveira Lira, cabol@ufpe.br
Universidade Federal de Pernambuco
Av. Prof Luiz Freire nº 1000
50740-540 Recife, PE. Brazil

Abstract. *The aim of this work is to solve the quasi incompressible two-dimensional Navier-Stokes equations, by means of a stabilized Finite Element Method (FEM). The mass conservation equation is re-written in order to obtain a relationship between the pressure and velocity fields. This is carried out by taking into account the existing relation between the fluid bulk modulus, the density and the pressure field. The energy equation, in its turn, is decoupled from the complete set of conservation equations. The resulting system is discretized with the aid of a streamline-upwind-Petrov-Galerkin Finite Element Method (SUPG). In this paper one makes use of a simple stabilization matrix. The numerical results obtained are quite consistent, in spite of the simplicity of the stabilization matrix employed. Numerical examples are presented and comparisons are made for validation purposes.*

Keywords: *Quasi incompressible flows, FEM, SUPG, Computational techniques*

1. INTRODUCTION

The fully incompressible fluid does not exist in nature. Even if the specific volume variation of a fluid subjected to a hydrostatic stress field may be really tiny, such a variation must occur.

If the bulk modulus is considered, we will be able to re-write the continuity equation so that a relation between pressure and velocity may be obtained. This approach has already been done, amongst others, by Brooks and Hughes (1982). Turkel et al. (1994) employ preconditioning techniques towards reaching the steady state. In this work, the bulk modulus is introduced in a rather natural way. Such quasi incompressible approach makes it possible to deal with a complex mathematical problem without losing physical significance in the final numerical results. This modified continuity equation, together with the momentum equation, establish a possible mathematical model for treating quasi incompressible flows.

With regard to the stabilization parameters, it is employed in this paper a quite simple form for them. Implementation of such simplified stabilizing terms avoids the use of numerical evaluation for them.

2. MATHEMATICAL BASIS

The incompressible Navier-Stokes equations in vector form are as follows:

$$\rho \frac{D\boldsymbol{u}}{Dt} = \rho \boldsymbol{f} - \nabla p + \mu \nabla^2 \boldsymbol{u} \tag{1}$$

$$\nabla^T \boldsymbol{u} = 0 \tag{2}$$

where ρ is density, D/Dt is the so-called material derivative operator, $\boldsymbol{f}$ is a body force field, ∇ is the gradient operator, p is pressure, μ is the fluid absolute viscosity, $\boldsymbol{u}$ is the velocity field, ∇^T is the divergence operator and ∇^2 is the Laplacian operator.

The fluid bulk modulus, in its turn, may be defined as follows:

$$k = \frac{\delta p}{(\frac{\delta \rho}{\rho})} \tag{3}$$

where p is pressure, ρ is density and δ stands for variation.

If we take into consideration Eq. (3) and the fact that mass is conserved, we can re-write Eq. (2) as follows:

$$\frac{1}{c^2}\frac{\partial p}{\partial t} + \rho \boldsymbol{\nabla}^T \boldsymbol{u} = 0 \tag{4}$$

where c is the speed of sound into the medium and t is time.

Equations (1) and (4) constitute themselves into the momentum and mass conservation equations employed in this paper. Equations (1) and (4) can be re-written in the following advective-diffusive form:

$$\boldsymbol{B}\boldsymbol{U}_{,t} + \frac{\partial \boldsymbol{F}^k}{\partial x_k} - \frac{\partial \boldsymbol{D}^k}{\partial x_k} - \boldsymbol{Q} = \boldsymbol{0} \tag{5}$$

with

$$\boldsymbol{B} = \begin{pmatrix} \boldsymbol{I}_{nd\times nd} & \boldsymbol{0}_{nd\times 1} \\ \boldsymbol{0}_{1\times nd} & (\frac{1}{\rho c^2}) \end{pmatrix} \tag{6}$$

where nd is the number of spatial dimensions;

$$\boldsymbol{U} = \begin{pmatrix} \boldsymbol{u}_{nd\times 1} \\ (\frac{p}{\rho}) \end{pmatrix} \tag{7}$$

is the fluid state vector;

x_k is the $k-th$ component of the position vector $\boldsymbol{x}$;

$$\boldsymbol{F}^k = \boldsymbol{A}_k \boldsymbol{U} \tag{8}$$

is the advective flux and $\boldsymbol{A}_k$ is the $k-th$ advective Jacobian, with $\boldsymbol{A}_k = \partial \boldsymbol{F}^k / \partial \boldsymbol{U}$ and $k = 1 \ to \ nd$;

$$\boldsymbol{D}^k = \boldsymbol{K}\boldsymbol{U}_{,x_k} \tag{9}$$

is the diffusive flux and $\boldsymbol{K}$ is the diffusive Jacobian:

$$\boldsymbol{K} = \begin{pmatrix} \nu \boldsymbol{I}_{nd\times nd} & \boldsymbol{0}_{nd\times 1} \\ \boldsymbol{0}_{1\times nd} & 0 \end{pmatrix} \tag{10}$$

where ν is the kinematic viscosity of the fluid.

Vector $\boldsymbol{Q}$ is:

$$\boldsymbol{Q} = \begin{pmatrix} \boldsymbol{f}_{nd\times 1} \\ 0 \end{pmatrix} \tag{11}$$

In this work, it will be assumed that $\boldsymbol{Q}$ is negligible as compared to the other terms in Eq. (5).

In addition to the symbols and notation introduced by Eqs. (6) through (11), a comma denotes operation of differentiation in Eq. (5). So, for instance, $_{,t}$ denotes a derivative with respect to time.

Position vector $\boldsymbol{x}$, with components x_k, $k = 1 \ to \ nd$, is defined in the spatial domain Ω, whereas time t is such that $t \in \left]0,T\right[$.

One must add the following initial and boundary conditions to Eq. (5):

$$U(t = 0) = U_0(\boldsymbol{x}) \tag{12}$$

$$\boldsymbol{U}(\boldsymbol{x},t) = \boldsymbol{U}_d \ , \ \forall \ (\boldsymbol{x},t) \in G^d \tag{13}$$

where $\boldsymbol{U}_d$ is a real vector such that $\boldsymbol{U}_d \in \mathbb{R}^{(nd+1)\times 1}$.

The last term in Eq. (13), namely G^d, stands for space-time boundary. The superscript d in Eq. (13) relates to the part of the boundary where the solution vector has been prescribed.

Consider now the following notations for the space-time domain R and its boundary G:

$$R = \Omega \times \left]0,T\right[\tag{14}$$

$$G = \Gamma \times \left]0,T\right[\tag{15}$$

In Equation (15), Γ stands for spatial boundary.

3. FINITE ELEMENT FORMULATION

In this paper, the finite element notations and finite element methodology employed by Costa and Lyra (2005) will be adopted.

Let the space-time domain R be partitioned, such that the following relation holds:

$$\hat{R}_n \equiv \sum_{e=1}^{N_e} (\hat{\Omega}_n^e) \times I_n \tag{16}$$

where a hat on top of a letter denotes approximation, n stands for time level and N_e stands for number of elements. Furthermore, in Eq. (16) $\hat{\Omega}_n^e$ is an approximate partition of the spatial domain at time level n. In its turn, I_n is a partition of the time sub-domain, as follows:

$$I_n = \left]t_n, t_{n+1}\right[\tag{17}$$

We will denote the spatial domain border and the element border as $\hat{\Gamma}_n$ and $\hat{\Gamma}_n^e$, respectively. As for the space-time borders, they will be referred to as G_n and G_n^e.

Consider now the following sets of functions:

$$S_n^h = \hat{\boldsymbol{U}} \mid \hat{\boldsymbol{U}} \in \left[C^0 \left(\hat{R}_n\right)\right]^{nd+1}, \ \hat{\boldsymbol{U}} = \boldsymbol{U}_d, \forall \ (\boldsymbol{x},t) \in \hat{G}_n^d \tag{18}$$

$$V_n^h = \hat{\boldsymbol{W}} \mid \hat{\boldsymbol{W}} \in \left[C^0 \left(\hat{R}_n\right)\right]^{nd+1}, \ \hat{\boldsymbol{W}} = \boldsymbol{0}, \ \forall \ (\boldsymbol{x},t) \in \hat{G}_n^d \tag{19}$$

where S_n^h is the discrete set of so-called trial or test functions, whereas V_n^h is a discrete space of so-called weighting functions.

It is considered in this paper the trial solution $\hat{\boldsymbol{U}}$ as being constant in time inside each R_n^e as defined by Eq. (16). In so doing, an approximate variational formulation can be written with regard to Eq. (5). Such approximate variational formulation can be stated as:

within each R_n *, find* $\hat{\boldsymbol{U}} \in S_n^h$ *such that for all* $\hat{\boldsymbol{W}} \in V_n^h$ *the following expression holds:*

$$\int_{\hat{\Omega}_n} \boldsymbol{W}^T \boldsymbol{B}(\hat{\boldsymbol{U}}_{n+1}-\hat{\boldsymbol{U}}_n)\, d\,\Omega - \int_{\hat{\Omega}_n}\int_{t_n}^{t_{n+1}} \frac{\partial \boldsymbol{W}^T}{\partial t}\hat{\boldsymbol{U}}\, dt\, d\,\Omega$$
$$- \int_{t_n}^{t_{n+1}}\int_{\hat{\Omega}_n} \frac{\partial \boldsymbol{W}^T}{\partial x_k}(\hat{\boldsymbol{F}}_{\boldsymbol{k}}-\hat{\boldsymbol{D}}_{\boldsymbol{k}})\, d\,\Omega\, dt \;+\; \int_{t_n}^{t_{n+1}}\int_{\hat{\Gamma}_n} [\boldsymbol{W}^T(\hat{\boldsymbol{F}}_{\boldsymbol{k}}-\hat{\boldsymbol{D}}_{\boldsymbol{k}})n_k]\, d\,\Gamma\, dt \;\equiv\; 0 \tag{20}$$

where n_k is the $k-th$ component of the unit outward normal vector to the boundary.

The SUPG weighting function $\boldsymbol{W}$ is to be written in the SUPG context as follows:

$$\boldsymbol{W} \;\equiv\; \sum_{i=1}^{N} (N_i \boldsymbol{I}_{(nd+1)\times(nd+1)} \;+\; (\boldsymbol{P}_i)_{(nd+1)\times(nd+1)})(\boldsymbol{w}_{\boldsymbol{i}})_{(nd+1)\times 1} \tag{21}$$

where N stands for the number of nodes into which the spatial domain is divided, $\boldsymbol{P}_i$ is the perturbation function, $\boldsymbol{w}_i$ is a vector of nodal constants and N_i is a constant-in-time and linear-in-space shape function for the node i .

In this work, we will make use of the $\boldsymbol{P}_i$ form given by Hughes and Mallet (1986):

$$\boldsymbol{P}_i \;\equiv\; \boldsymbol{A}_k \frac{\partial N_i}{\partial x_k}\boldsymbol{\tau} \tag{22}$$

Matrix $\boldsymbol{\tau}$ in Eq. (22) is the so-called matrix of intrinsic times in SUPG terminology. Employing the weighting function expressed by Eq. (21) with $\boldsymbol{P}_i$ being given by Eq. (22), it is possible to reach the following approximate variational equation:

$$\int_{\hat{\Omega}_n} N_i \boldsymbol{B}(\hat{\boldsymbol{U}}_{n+1}-\hat{\boldsymbol{U}}_n)\, d\,\Omega - (\Delta t)\int_{\hat{\Omega}_n} \frac{\partial N_i}{\partial x_k}(\hat{\boldsymbol{F}}_{\boldsymbol{k}}-\hat{\boldsymbol{D}}_{\boldsymbol{k}})\, d\,\Omega$$
$$+\;(\Delta t)\int_{\hat{\Gamma}_n} N_i(\hat{\boldsymbol{F}}_{\boldsymbol{k}}-\hat{\boldsymbol{D}}_{\boldsymbol{k}})n_k\, d\,\Gamma + (\Delta t)\sum_{e=1}^{N_e}\int_{\hat{\Omega}_n^e} \boldsymbol{A}_k \frac{\partial N_i}{\partial x_k}\boldsymbol{\tau}\boldsymbol{A}_h \frac{\partial \boldsymbol{U}}{\partial x_h}\, d\,\Omega \;\equiv\; \boldsymbol{0} \tag{23}$$

The usual FEM expansion is now re-called for expressing trial function $\hat{\boldsymbol{U}}$:

$$\hat{\boldsymbol{U}} \;=\; \sum_{j=1}^{N} N_j \hat{\boldsymbol{u}}_j \tag{24}$$

where N_j is a *constant-in-time* and *linear-in-space* shape function for the node j , N stands for the number of knots into which the spatial domain is divided and $\hat{\boldsymbol{u}}_j$ are constant nodal vectors.

Re-writing of Eq. (23) by considering Eq. (24) yields:

$$\int_{\hat{\Omega}_n} N_i N_j \boldsymbol{B}(\hat{\boldsymbol{u}}_{n+1}-\hat{\boldsymbol{u}}_n)\, d\,\Omega - (\Delta t)\int_{\hat{\Omega}_n} \frac{\partial N_i}{\partial x_k}(\hat{\boldsymbol{F}}^k_{(n+1)}-\hat{\boldsymbol{D}}^k_{(n+1)})\, d\,\Omega$$
$$+\;(\Delta t)\int_{\hat{\Gamma}_n} N_i(\hat{\boldsymbol{F}}^k_{(n+1)}-\hat{\boldsymbol{D}}^k_{(n+1)})n_k\, d\,\Gamma + (\Delta t)\sum_{e=1}^{N_e}\int_{\hat{\Omega}_n^e} \boldsymbol{A}_k \frac{\partial N_i}{\partial x_k}\boldsymbol{\tau}\boldsymbol{A}_h \frac{\partial N_j}{\partial x_h}\hat{\boldsymbol{u}}_{(n+1)}\, d\,\Omega \;\equiv\; \boldsymbol{0} \tag{25}$$

In Equation (25), subscripts k and h refer to the spatial co-ordinate, whereas i and j refer to the number of the node. Equation (25) can then be written in the following fashion:

$$\boldsymbol{\Pi}(\hat{\boldsymbol{u}}_{(n+1)},\ \hat{\boldsymbol{u}}_n) = \mathbf{0} \tag{26}$$

where $\boldsymbol{\Pi}$ is the functional on the left hand-side of Eq, (25).

One possible way of solving Eq. (26) is by means of a *Predictor-Multicorrector* algorithm. Such an algorithm enables us to obtain the solution at time level $n+1$, if we possess its value at time level n. This is possible via solution of a system of linear equations with the following form:

$$\frac{\partial \boldsymbol{\Pi}(\hat{\boldsymbol{u}}_i^{(n+1)},\ \hat{\boldsymbol{u}}^n)}{\partial \hat{\boldsymbol{u}}_i^{n+1}}(\hat{\boldsymbol{u}}_{i+1}^{n+1} - \hat{\boldsymbol{u}}_i^{n+1}) \approx -\boldsymbol{\Pi}(\hat{\boldsymbol{u}}_i^{n+1},\ \hat{\boldsymbol{u}}^n) \tag{27}$$

where $\hat{\boldsymbol{u}}_i^{(n+1)}$ is the $i-th$ guess on the solution $\hat{\boldsymbol{u}}^{(n+1)}$ and $\hat{\boldsymbol{u}}_{(i+1)}^{(n+1)}$ is its improved value obtained through solution of the linear system (27).

The very first term on the left member of Eq. (27), i.e., the derivative of $\boldsymbol{\Pi}$ with respect to $\hat{\boldsymbol{u}}_i^{(n+1)}$ is a matrix which can be decomposed as a sum of elementary matrices as follows:

$$\frac{\partial \boldsymbol{\Pi}(\hat{\boldsymbol{u}}_i^{(n+1)},\ \hat{\boldsymbol{u}}^n)}{\partial \hat{\boldsymbol{u}}_i^{n+1}} = \boldsymbol{B}(\boldsymbol{a}_M)_e + (\Delta t)[\boldsymbol{a}_e + (\boldsymbol{a}_{PG})_e + (\boldsymbol{a}_h)_e] \tag{28}$$

where subscripts e stand for "element".

As a standard procedure when operating in the context of the Finite Element Method, the computation of each term on the right member of Eq. (28) can be carried out in an elementwise fashion. If we denote the number of nodes in an element by N_c, then the resulting element matrices on the right member of Eq. (28) have dimension $[N_c\times(nd+1)]\times[N_c\times(nd+1)]$. Furthermore, re-calling it is being used linear shape functions in this work, it may be written what follows:

$$(\boldsymbol{a}_M)_e(i,j) = [\int_{\hat{\Omega}_e^n} N_i N_j d\,\Omega]\boldsymbol{I} \tag{29}$$

$$(\boldsymbol{a})_e(i,j) = (\boldsymbol{A}_k \frac{\partial N_j}{\partial x_k})\int_{\hat{\Omega}_e^n} N_i\, d\,\Omega \tag{30}$$

$$(\boldsymbol{a}_{PG})_e(i,j) = (\boldsymbol{A}_k \boldsymbol{\tau} \frac{\partial N_i}{\partial x_k})(\boldsymbol{A}_h \frac{\partial N_j}{\partial x_h})\int_{\hat{\Omega}_e^n} d\,\Omega \tag{31}$$

$$(\boldsymbol{a}_h)_e(i,j) = \frac{\partial N_i}{\partial x_k}(\boldsymbol{K}\frac{\partial N_j}{\partial x_h})\int_{\hat{\Omega}_e^n} d\,\Omega \tag{32}$$

To complete this formulation, we need to make the form of the $\boldsymbol{\tau}$ matrix explicit. The form of the $\boldsymbol{\tau}$ matrix used in this paper is the following:

$$\boldsymbol{\tau} \equiv diag\{\tau_{11},\ \tau_{22},\ \tau_{33}\} \tag{33}$$

where

$$\tau_{11} = \frac{h_e}{2} \tag{34}$$

$$\tau_{22} = \frac{h_e}{2}\frac{1}{(|\boldsymbol{u}_e^2| + 2)^{\frac{1}{2}}} \tag{35}$$

$$\tau_{33} = \frac{h_e}{2}\frac{1}{(|\boldsymbol{u}_e^2| + 1)^{\frac{1}{2}}} \tag{36}$$

where h_e is a characteristic dimension of the element which can be, for two-dimensional problems, the square root of the element area. As for $|\boldsymbol{u}_e|$, it stands for the euclidean norm of the element velocity vector $\boldsymbol{u}_e$.

4. NUMERICAL RESULTS

The problem of the lid-driven cavity was used as a test for the formulation presented in the previous section. Figure (3) depicts the cavity in itself as well as the mesh employed for simulating its flows.

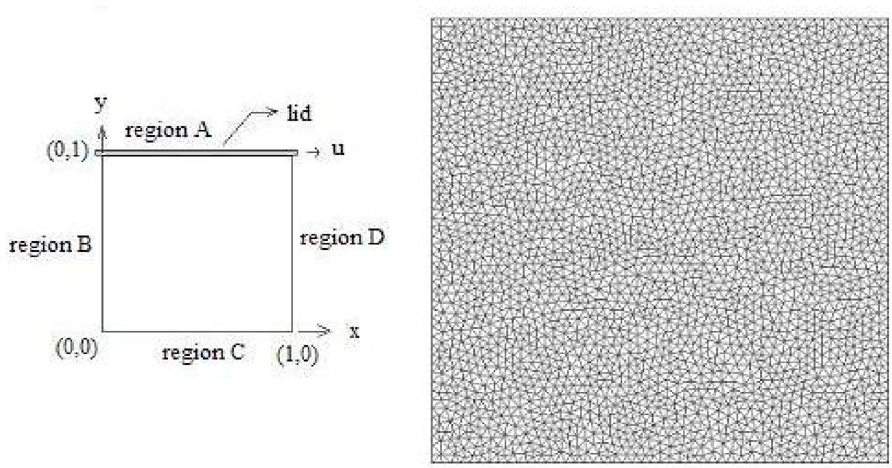

Figure 1: Cavity sketch (left) and its related mesh (right).(out of scale)

In Figure (3), left, u denotes the magnitude of the lid velocity vector, which was taken as $u = 1\ m/s$ in this work. With regard to the co-ordinate system shown in Fig. (3), left, the lid velocity vector has the form $\boldsymbol{u} = [u,0,0]^T$. This is precisely the boundary condition regarding region A in Fig. (3), left. As for regions B, C and D of Fig.(3), left, the boundary condition is that of non-slipping one, i.e., $\boldsymbol{u} = \boldsymbol{0}\ m/s$. The final boundary condition involves pressure and is $p(x = 0.5m,\ y = 0m) = 0N/m^2$. The initial condition, in its turn, was taken as $p(t = 0s) = 0N/m^2$ and $\boldsymbol{u}(t = 0s) = \boldsymbol{0}\ m/s$. There should be noticed that there is a singularity on both left and right top corners of the cavity with respect to the definitions of velocity. To circumvent such a difficulty, we deal with such a singularity in this paper just as, for instance, Lyra (1994) or Costa (2004) did. It was then prescribed a linear velocity distribution for those top corners regions. If we use *linear-in-space* shape functions, as it is the case in this paper, assumption of a linear velocity distribution for the regions described above amounts to prescribing the velocity vector on both left and right top corners of the cavity as $\boldsymbol{u} = [u,0,0]^T$. With regard to the knots placed on the vertical walls of the cavity, namely regions B and D, and right below the top corner knots, it was prescribed velocity vector as $\boldsymbol{u} = \boldsymbol{0}\ m/s$. The problem mesh can be seen in Fig. (1), right. The uniform, unstructured mesh seen in Fig. (1), right, contained 5227 linear triangular elements and 2712 nodes. The reference literature employed for purposes of comparison was Ghia et al. (1982).

We simulated flows with three different Reynolds numbers, namely $R_e = 100$, $R_e = 1000$ and $R_e = 5000$. Plots were done where we can see the value of the u_2 component of the velocity field as a function of the abcissa x for ordinate y being kept constant and equal to $0.5\ m$ for each of the Reynolds numbers considered. Likewise, plots were drawn where we can see the value of the u_1 component of the velocity field as a function of the ordinate y for abcissa x being kept constant and equal to $0.5\ m$ for each of the Reynolds numbers considered. Figures (2) through (4) show such plots.

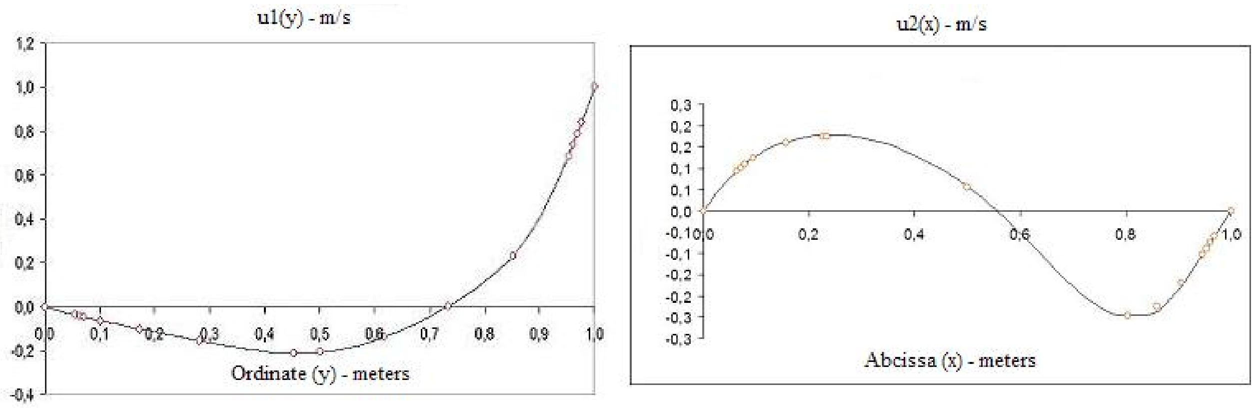

Figure 2: Lid driven cavity - Reynolds 100

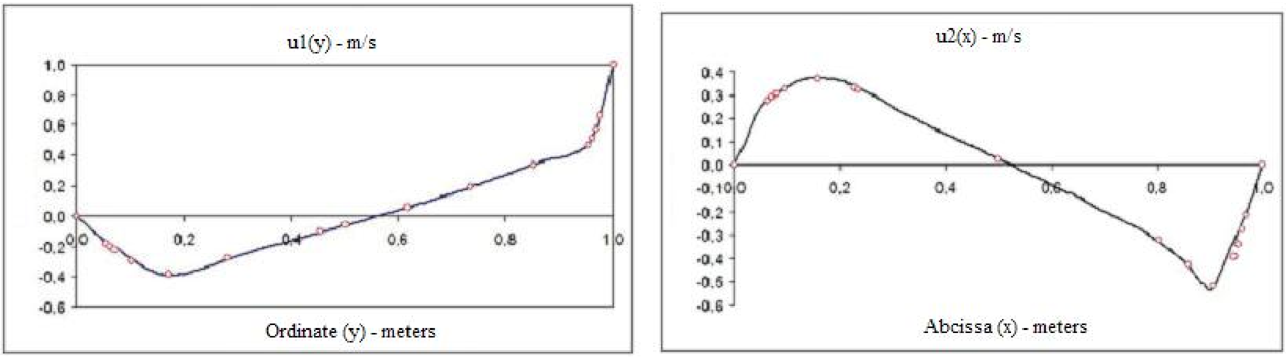

Figura 3: Lid driven cavity - Reynolds 1000

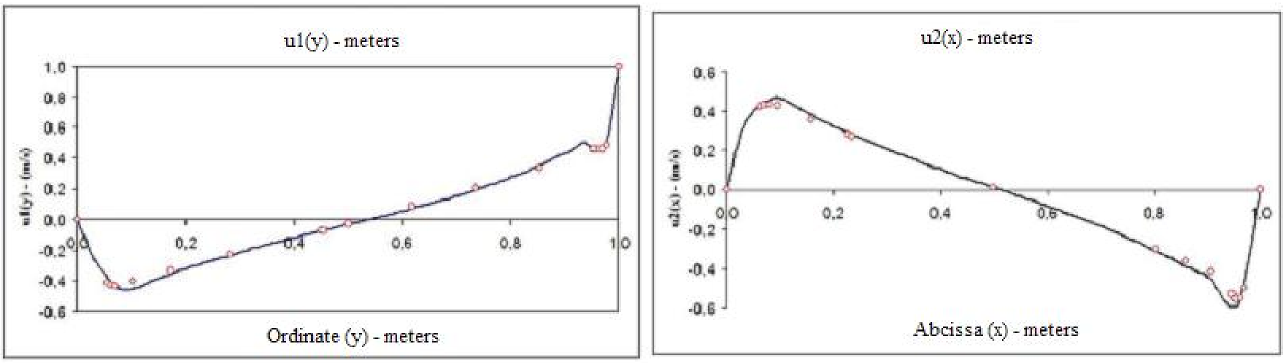

Figure 4: Lid driven cavity - Reynolds 5000

In Figs. (2) through (4), the small-sized, colored circles represent the values obtained by Ghia et al. (1982). Curves in black represent the data obtained in this work. As it can be seen from Figs.(2) through (4), there was good agreement between the results published by Ghia et al. (1982) and ours, for all the Reynolds numbers considered. Figure (5) shows the pressure isolines obtained in this work for the considered Reynolds numbers.

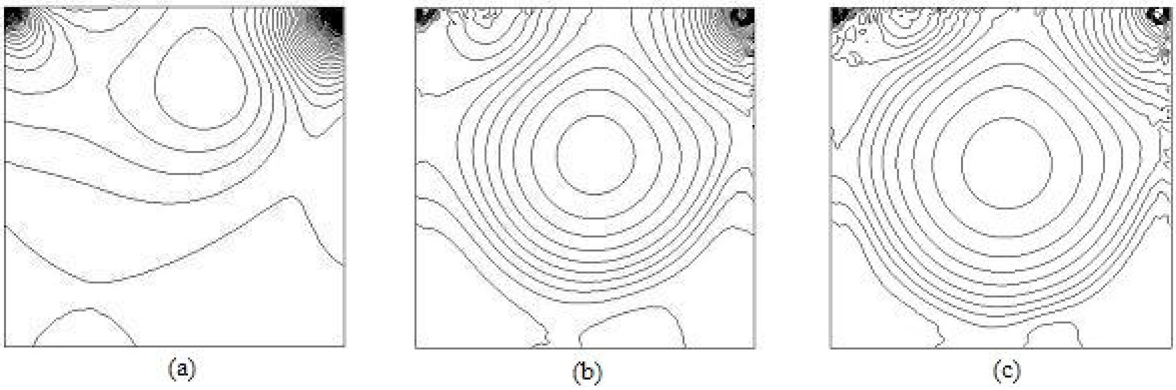

Figure 5: Lid driven cavity - pressure isolines for Re = 100 (a), Re = 1000 (b) and for Re = 5000 (c)

5. CONCLUSIONS

An SUPG Finite Element Method was shown to solve the quasi incompressible Navier-Stokes equations. Although the stabilizing matrix presented was quite simple, the numerical results showed the robustness of the formulation to cope with rather complex problems such the lid driven cavity one. Further work might address, for instance, the description of turbulence for quasi incompressible fluid flows.

3. ACKNOWLEDGEMENTS

The authors would like to thank the Brazilian Research Council (CNPq) for the financial support granted.

4. REFERENCES

Brooks, N. and Hughes, T.J.R., "Streamline Upwind / Petrov-Galerkin fomulations for convection dominated flows with particular emphasis on the incompressible Navier-Stokes equations**"**. Computer Methods in Applied Mechanics and Engineering, USA, 32: 199-259, 1982.

Turkel, E.; Fiterman, A; Van Leer, B., "Preconditioning and the limit of the compressible to the incompressible flow equations for finite difference schemes". In: Caughey, D.A.; Hafez, M.M. (Eds.). Frontiers of computational fluid dynamics**.** [S.L]: John Wiley & Sons, 1994, 215-234.

Costa, G.K. and Lyra, P.R.M., "A stabilized finite element formulation to solve high and low speed flows." Communications in numerical methods in engineering, 2006, 22: 411-419.

Hughes, T.J.R. and Mallet, M., "A new finite element formulation for computacional fluid dynamics: III. The generalized streamline operator for multidimensional advective-diffusive systems**.**" Computer Methods in Applied Mechanics and Engineering, USA, 58: 305-328, 1986.

Costa, G.K., "Simulação tridimensional de escoamentos compressíveis e incompressíveis através do método dos elementos finitos**",** 2004. 175p. (Doctoral Thesis – Universidade Federal de Pernambuco, Recife – Brasil).

Lyra, P.R.M., "Unstructured grid adaptive algorithms for fluid dynamics and heat conduction"**.** Swansea, 1994. 333 p. (Doctoral Thesis – University of Wales, Swansea – United Kingdom).

Ghia, U.; Ghia, K.N. and Shin, C.T., "High-Re Solutions for Incompressible Flow Using the Navier-Stokes Equations and a Multigrid Method**"**. Journal of Computational Physics, 48: 387-411, 1982.

5. RESPONSIBILITY NOTICE

The authors are the only responsible for the printed material included in this paper.